Robust Statistical Ranking: Theory and Algorithms

Qianqian Xu†, Jiechao Xiong†, Qingming Huang, *Senior Member, IEEE,* and Yuan Yao‡

Abstract—Deeply rooted in classical social choice and voting theory, statistical ranking with paired comparison data experienced its renaissance with the wide spread of crowdsourcing technique. As the data quality might be significantly damaged in an uncontrolled crowdsourcing environment, outlier detection and robust ranking have become a hot topic in such data analysis. In this paper, we propose a robust ranking framework based on the principle of Huber's robust statistics, which formulates outlier detection as a LASSO problem to find sparse approximations of the cyclic ranking projection in Hodge decomposition. Moreover, simple yet scalable algorithms are developed based on Linearized Bregman Iteration to achieve an even less biased estimator than LASSO. Statistical consistency of outlier detection is established in both cases which states that when the outliers are strong enough and in Erdös-Rényi random graph sampling settings, outliers can be faithfully detected. Our studies are supported by experiments with both simulated examples and real-world data. The proposed framework provides us a promising tool for robust ranking with large scale crowdsourcing data arising from computer vision, multimedia, machine learning, sociology, etc.

Index Terms—Crowdsourcing; Paired Comparison; Robust Ranking; Robust Statistics; Outlier Detection; Linearized Bregman Iteration; Hodge Decomposition; Random Graph

arXiv:1408.3467v1 [stat.ME] 15 Aug 2014

1 INTRODUCTION

Statistical preference aggregation, in particular ranking or rating from pairwise comparisons, is a classical problem which can be traced back to the 18^{th} century. This subject area has been widely studied in various fields including the social choice or voting theory in Economics [13], [43], Psychology [52], [44], Statistics [7], [35], [25], [11], Computer Vision [22], [38], [65], [66], [33], Information Retrieval [8], [32], Machine Learning [10], [41], and others [50], [47], [37]. Recently pairwise ranking methods gain a new surge of rapid growth with the wide spread of crowdsourcing platforms (e.g., MTurk, Innocentive, CrowdFlower, CrowdRank, and Allourideas), which enables low cost data collection with a large number of voters.

Methods for rating/ranking via pairwise comparison in crowdsourcing scenario must address a number of inherent difficulties including: (i) incomplete and imbalanced data; (ii) conflicts of interests or inconsistencies in the data; (iii) online and streaming data; (iv) outlier detection. Among various approaches, recently a Hodge-theoretic approach to statistical ranking [29], also called HodgeRank here, is able to characterize the intrinsic inconsistency in paired comparison data geometrically while infering a global ranking from incomplete and imbalanced samples, as a generalization of classical Borda Count in voting theory [12]. Such a methodology has been rapidly applied to the crowdsourced assessment for quality of experience (QoE) in multimedia, together with random graph models of sampling design [61], [59], which is favored in crowdsourcing studies where individuals provide the ratings in more diverse and less controlled settings than traditional lab environment [16]. Equipped with recent new developments on topological random graph theory in mathematics [30], [31], the framework, HodgeRank on Random Graphs, enables us to derive the constraints on sampling complexity to which the random selection must adhere. Instead of pursuing a quadratic number of pairs $\binom{n}{2} \approx n^2$ in a complete paired comparison design for n candidates, Erdös-Rényi random graph designs only need almost linear $O(n \log n)$ distinct sample pairs to ensure the graph connectivity for inferring a global ranking score and $O(n^{3/2})$ pairs to ensure the loop-free clique complex to avoid global inconsistency measured by harmonic ranking. Moreover, it allows an extension to online sampling settings. In [60], [63], some online algorithms are proposed based on the classic Robbins-Monro procedure [42] or stochastic gradient method for HodgeRank on random graphs, together with online tracking of topological evolution of paired comparison complex. For every edge independent sampling process, the online algorithm for global rating scores reaches minimax optimal convergence rates hence asymptotically as efficient as a batch algorithm, when dealing with streaming or large-scale data.

- *Q. Xu is with BICMR, Peking University, Beijing 100871, China, (email: xuqianqian@math.pku.edu.cn).*
- *J. Xiong and Y. Yao are with BICMR-LMAM-LMEQF-LMP, School of Mathematical Sciences, Peking University, Beijing 100871, China, (email: xiongjiechao@pku.edu.cn; yuany@math.pku.edu.cn).*
- *Q. Huang is with the University of Chinese Academy of Sciences & Institute of Computing Technology of Chinese Academy of Sciences, Beijing 100190, China, (email: qmhuang@jdl.ac.cn).*

†*Equally contribution to this work.*
‡*Corresponding author.*

Despite of these charming features, not all the data in crowdsourcing experiments are trustworthy. Due to the lack of supervision when subjects perform experiments in crowdsourcing, they may provide erroneous responses perfunctorily, carelessly, or dishonestly [9]. For example, when the testing time for a single participant lasts too long, the participant may become impatient and may input random decisions. Such random decisions are useless and may deviate significantly from other raters' decisions. Since the inference of global ranking score in HodgeRank depends on a least square problem, it may be fragile against such outliers.

In crowdsourcing study of multimedia [9], [57], Transitivity Satisfaction Rate (TSR) is proposed for outlier detection, which checks all the intransitive (circular) triangles such that $A \succ B \succ C \succ A$ where $\succ$ indicates preference. The TSR is defined as the number of transitive judgment triplets divided by the total number of triplets where transitivity may apply. However, TSR can only be applied for complete and balanced paired comparison data. When the paired data are incomplete, i.e., have missing edges, the question remains open of how to detect the noisy pairs.

On the other hand, some ranking methods have been seen robust against sparse and uniform outliers, such as angular embedding [46], [66], where [58] has shown that it has the same kind of phase transition in global ranking reconstruction as L1-norm ranking but only approximately recovers the ranking score. Furthermore, there has been a long history in robust statistics [28] which has not been investigated in this scenario.

In this paper, we fill in this gap by presenting a simple scheme starting from a LASSO [53] reformulation of Huber's robust regression [28]. Under this scheme, outlier detection becomes a sparse approximation of cyclic ranking component in the Hodge decomposition of paired comparison data, a characterization of total inconsistency or conflicts of interests. To meet the future challenge of big data analysis in crowdsourcing era, we develop a simple yet efficient and easy-to-parallelize algorithm for outlier detection based on Linearized Bregman Iteration (LBI).

Our contributions in this work are highlighted as follows:

(A) A Huber-LASSO framework is proposed for outlier detection and global ranking inference, where the outliers are sparse approximation of cyclic ranking projection in Hodge decomposition.
(B) Some scalable algorithms are proposed based on Linearized Bregman Iteration which is less biased than LASSO and suitable for large scale analysis.
(C) Statistical consistency for outlier detection is established with both Huber-LASSO and Linearized Bregman Iteration.
(D) The effectiveness of the proposed methodology is demonstrated on both simulated examples and real-world data.

This paper is an extension of our conference paper [62], which formulates the outlier detection as a LASSO problem. Regularization paths of LASSO could provide us an order on samples tending to be outliers. However, the computational cost of full LASSO path is prohibitive from the applications of large scale crowdsourcing problem. As a departure from the previous work, in this paper, we consider the Linearized Bregman Iteration for outlier detection, which is motivated by some differential equation (or more precisely, inclusion) approach to remove bias in LASSO paths and allows extremely simple and fast implementation for large scale problems.

The remainder of this paper is organized as follows. Section 2 contains a review of related work. Then we systematically introduce the theory and fast algorithms for robust statistical ranking, based on Huber-LASSO and Linearized Bregman Iterations in Section 3. Statistical consistency theory for both cases is established in Section 4. Detailed experiments are presented in Section 5, followed by the conclusions in Section 6.

2 RELATED WORK

2.1 Statistical Ranking

In pairwise ranking aggregation, there is a set of n elements to rank, and one is given outcomes of various pairwise comparisons among these elements; the goal is to aggregate these pairwise comparisons into a global ranking over the elements. Various algorithms have been studied for this problem, including maximum likelihood under a Bradley-Terry model assumption, rank centrality (PageRank/MC3) [34], [15], least squares (HodgeRank [29]) , and a pairwise variant of Borda count [12] among others. These methods have been widely used in surface reconstruction [22], shape from shading [26], high dynamic range compression [21], image matting and fusion [3], image and video quality assessment [61], [59], and various model fitting scenarios [40], [6].

If we consider the setting where pairwise comparisons are drawn I.I.D. (i.e., independently and identically distributed) from some fixed but unknown probability distribution, under a "time-reversibility" condition, the rank centrality (PageRank) and HodgeRank algorithms both converge to an optimal ranking [41]. However, PageRank is only able to aggregate the pairwise comparisons into a global ranking over the items. HodgeRank not only provides us a mean to determine a global ranking from paired comparison data under various statistical models (e.g., Uniform, Thurstone-Mosteller, Bradley-Terry, and Angular Transform), but also measures the inconsistency of the global ranking obtained. In particular, it takes a graph theoretic view, which maps paired comparison

data to edge flows on a graph, possibly imbalanced (where different pairs may receive different number of comparisons) and incomplete (where every participant may only provide partial comparisons), and then applies combinatorial Hodge Theory to achieve an orthogonal decomposition of such edge flows into three components: gradient flow for global rating (optimal in the L2-norm sense), triangular curl flow for local inconsistency, and harmonic flow for global inconsistency. Such a perspective provides us with a universal geometric description of the structure of paired comparison data, which may help understand various models, in particular the linear models with sparse outliers used in this paper.

As HodgeRank solves the global ranking score via a graph Laplacian linear equation, it benefits greatly from such a structure – not only fast algorithms exist for such problems [48], but also various random graph models can be exploited [61], [59], such as the Erdös-Rényi random graph [18], random regular graph [56], preferential attachment random graph [4], small world random graph [55], and geometric random graph [39].

2.2 Outlier Detection and Robust Statistics

Outliers are also referred to as abnormalities, discordants, deviants, or anomalies in the computer science and statistics literature. It is typically defined to be data samples which have an unusual deviation from the most common or expected pattern. Outliers are rare events, but once they have occurred, they may lead to a large instability of models estimated from the data. Therefore, outlier detection is a critical task in many fields and has been explored for a long time, especially in statistics [28]. However, there is no universal approach that is applicable in all settings. In this paper, we adopt a statistical linear model for the paired comparison data, namely HodgeRank model [59], and consider additive sparse outliers as they recently appeared in a variety of different studies [33], [66], [58], [62].

Various methods have been developed in literature for outlier detection and robust statistics. Among these studies, perhaps the most well-known one is robust regression with Huber's loss [28], which combines the least squares and the least absolute deviation problems. Recently, [23] discovered that robust regression with Huber's loss is equivalent to a LASSO problem, which leads to a new understanding of outlier detection based on modern variable selection techniques, e.g., [45].

2.3 Linearized Bregman Iteration

Linearized Bregman Iteration (LBI) was firstly introduced in [64] in the literature of variational imaging and compressive sensing. It is well-known that LASSO estimators are always biased [19]. On the other hand, [49] notices that Bregman iteration may reduce bias, also known as contrast loss, in the context of Total Variation image denoising. Now LBI can be viewed as a discretization of differential equations (inclusions) which may produce unbiased estimators under nearly the same model selection consistency conditions as LASSO [36].

Beyond such a theoretical attraction, LBI is an extremely simple algorithm which combines an iterative gradient descent algorithm together with a soft thresholding. It is different to the well-known iterative soft-thresholding algorithm (ISTA) (e.g., [14], [5] and references therein) which converges to the biased LASSO solution. To tune the regularization parameter in noisy settings, one needs to run ISTA with many different thresholding parameters and chooses the best among them; in contrast, LBI only runs in a single path and regularization is achieved by early stopping like boosting algorithms [36], which may save the computational cost greatly and thus suitable for large scale implementation, e.g., distributive computation [67].

3 Robust HodgeRank

In this section, we systematically introduce the theory and fast algorithms for robust statistical ranking, based on Huber-LASSO and Linearized Bregman Iterations. Specifically, we first start from a basic linear model with different types of noise models, which have been successfully used widely in literature. Second, a Huber-LASSO framework is introduced such that outlier detection becomes sparse cyclic approximation in Hodge Decomposition of pairwise ranking data. Various techniques from robust statistics and LASSO can be used here. Finally we introduce some scalable algorithms using linearized Bregman iterations.

3.1 Basic Linear Model

Let $\wedge$ be a set of raters and $V = \{1, ..., n\}$ be the set of items to be ranked. Paired comparison data is collected as a real-valued function with missing values, $\wedge \times V \times V \rightarrow \mathbb{R}$, which is *skew-symmetric* for each $\alpha \in \wedge$, i.e., $Y_{ij}^{\alpha} = -Y_{ji}^{\alpha}$ representing the degree that rater α prefers i to j. Without loss of generality, one assumes that $Y_{ij}^{\alpha} > 0$ if α prefers i to j and $Y_{ij}^{\alpha} \leq 0$ otherwise. The choice of scale for Y_{ij}^{α} varies in applications. For example, in multimedia quality of experience assessment [61], dichotomous choice $\{\pm 1\}$ or a k-point Likert scale ($k = 3, 4, 5$) are often used; while in machine learning [10] and surface reconstruction [66] etc., general real values are assumed.

In this paper, consider the following linear model:

$$Y_{ij}^{\alpha} = \theta_i^* - \theta_j^* + z_{ij}^{\alpha}, \tag{1}$$

where $\theta^* \in \mathbb{R}^V$ is some true scaling score on V and z_{ij}^α are noise.

Paired comparison data above can be mapped to edge flows on a graph $G = (V, E)$ where the edge set E consists of all pairs of items $\{i, j\}$ which are comparable in data. Define the gradient operator (finite difference operator) [29], [61] on graph G by $\delta_0 : \mathbb{R}^V \to \mathbb{R}^E$ such that $(\delta_0\theta)(i, j) = \theta_i - \theta_j$, then one can rewrite (1) as

$$Y = X\theta^* + z, \tag{2}$$

where the design matrix $X = \delta_0$ and the Gram matrix $L_0 = X^T X$ becomes the unnormalized Graph Laplacian. In this way, $X\theta^*$ can be viewed as a gradient flow induced by a potential/scaling function $\theta^* : V \to \mathbb{R}$, and the measurement Y is contaminated by noise z. We assume that the graph G is connected such that its graph Laplacian L_0 has rank $n - 1$.

Now we are going to present some noise models $z \sim F_z$ which are often met in practice.

3.1.1 Gaussian-type noise

If $z_{ij}^\alpha = \varepsilon_{ij}^\alpha$ represents independent noise with mean zero and fixed variance, the Gauss-Markov theorem tells us that the unbiased estimator with minimal variance is given by the least squares problem (L2),

$$\min_{\sum_{i\in V}\theta_i=0} \sum_{i,j,\alpha} (\theta_i - \theta_j - Y_{ij}^\alpha)^2. \tag{3}$$

whose estimator solves the Graph Laplacian equation $L_0\theta = div(Y) := \delta_0^T Y$. Such an algorithm has been used in [61], [59], [60] to derive scaling scores in subjective multimedia assessment.

3.1.2 Gaussian Noise with Outliers

However, not all comparisons are trustworthy and there may be sparse outliers. Putting in a mathematical way, here we consider

$$z_{ij}^\alpha = \gamma_{ij}^\alpha + \varepsilon_{ij}^\alpha, \tag{4}$$

where outlier γ_{ij}^α has a much larger magnitude than ε_{ij}^α and is sparse in the sense that most of its elements are zeroes.

How can one modify least squares problem to achieve a robust estimator against sparse outliers?

3.2 Huber-LASSO

To deal with different types of noises, Huber [27], [28] proposes the following robust regression,

$$\min_{\sum_{i\in V}\theta_i=0} \sum_{i,j,\alpha} \rho(\theta_i - \theta_j - Y_{ij}^\alpha), \tag{5}$$

where $\rho : \mathbb{R} \to [0, \infty)$ is a differentiable convex function with derivative $\psi(x) = \rho'(x)$. For fixed number of items n, as the number of paired comparisons m satisfies $n/m \to 0$, a solution of (5) satisfies asymptotically $\hat{\theta} \sim N(0, \Sigma)$ where $\Sigma = V(\psi, F_z)L_0^\dagger$ and $V(\psi, F_z) = \mathbb{E}[\psi^2]/(\mathbb{E}[\psi'])^2$. Had we known the density of noise $dF_z(x) = f_z(x)dx$, the optimal choice of ρ would be decided by $\psi(x) = (\log f_z(x))'$ such that the asymptotic variance meets the lower bound via the Fisher information, i.e., $V(\psi, F_z) = 1/I(F_z)$. Square loss is hence an optimal choice for Gaussian noise. Note that in high dimensional settings $n/m \to c > 0$, the asymptotic variance gets more complicated [17], which leaves us a new favorite consideration on random graph designs in paired comparison experiments [61], [59]. Erdös-Rényi random graphs are almost surely connected as long as $m \gg n \log n$, so $n/m \to 0$.

However noise model (4) contains singularities as outliers, hence one can't derive an optimal convex ρ as above. Nevertheless the Huber's loss function ρ_λ is a good choice for ρ

$$\rho_\lambda(x) = \begin{cases} x^2/2, & \text{if } |x| \le \lambda \\ \lambda|x| - \lambda^2/2, & \text{if } |x| > \lambda. \end{cases}$$

It is a strongly convex and smooth function. When $|\theta_i - \theta_j - Y_{ij}^\alpha| < \lambda$, the comparison is regarded as a "good" one with Gaussian noise and L2-norm penalty is used on the residual. Otherwise, it is regarded as a "bad" one contaminated by outliers and L1-norm penalty is applied which is less sensitive to the amount of deviation. So when $\lambda = 0$, it reduces to a least absolute deviation (LAD) problem or L1-norm ranking [37].

Huber's robust regression (5) with ρ_λ is equivalent to the following LASSO formulation [62]:

$$\begin{aligned} &\min_{\sum_{i\in V}\theta_i=0,\gamma} \tfrac{1}{2}\|Y - X\theta - \gamma\|_2^2 + \lambda\|\gamma\|_1 \\ &:= \textstyle\sum_{i,j,\alpha}[\tfrac{1}{2}(\theta_i - \theta_j + \gamma_{ij}^\alpha - Y_{ij}^\alpha)^2 + \lambda|\gamma_{ij}^\alpha|] \quad . \end{aligned} \tag{6}$$

To see this, let $(\hat{\theta}^{lasso}, \hat{\gamma}^{lasso})$ be a solution of (6). Here we introduce a new variable γ_{ij}^α for each comparison Y_{ij}^α such that $|\gamma_{ij}^\alpha| > 0$ is equivalent to $|\hat{\theta}_i^{lasso} - \hat{\theta}_j^{lasso} - Y_{ij}^\alpha| > \lambda$, i.e., an outlier. To be less sensitive to outliers, an L1-norm penalty of $\gamma_{ij}^\alpha = \hat{\theta}_i^{lasso} - \hat{\theta}_j^{lasso} - Y_{ij}^\alpha$ is used as in Huber's loss [28]. Otherwise, an L2-norm is used to attenuate the Gaussian noise. This optimization problem is a partially penalized LASSO [53], hence called Huber-LASSO (or HLASSO) in this paper.

Standard LASSO packages such as `glmnet` and `quadrupen` do not solve HLASSO (6) directly. Fortunately HLASSO can be split into two subproblems with the two groups of variables decoupled, via orthogonal projections of data Y onto the column space of X and its complement. In particular, the outlier γ is involved in a standard LASSO problem, whose design matrix comes from the projection onto the complement of the column space of X.

To see this, let X has a full SVD decomposition $X = U\Sigma V^T$ and $U = [U_1, U_2]$ where U_1 is an orthonormal basis of the column space $\mathrm{col}(X)$ and U_2 becomes an orthonormal basis for $\ker(X^T)$. Then the following result provides a precise statement of the split of HLASSO.

Proposition. The HLASSO solution $(\hat{\theta}, \hat{\gamma})$ can be obtained by the following two problems

$$\min_{\gamma} \frac{1}{2}\|U_2^T Y - U_2^T \gamma\|_2^2 + \lambda\|\gamma\|_1 \tag{7}$$

$$\min_{\sum_{i\in V}\theta_i=0} \frac{1}{2}\|U_1^T X\theta - U_1^T(Y-\hat{\gamma})\|_2^2. \tag{8}$$

Note that

$$U_2U_2^T = I - U_1U_1^T = I - X(X^TX)^\dagger X^T, \tag{9}$$

where $A^\dagger$ denotes the Moore-Penrose inverse of A. Hence we do not need the full SVD to solve (7).

Hence the original HLASSO is split into two separate optimization problems: the first in (7) is a standard LASSO problem which detects outliers and the second in (8) is a least squares problem which calculates scores via corrected data $Y - \hat{\gamma}$.

3.2.1 Outliers as Sparse Cyclic Approximation in Hodge Decomposition

The algorithm proposed above admits a neat interpretation from Hodge Decomposition for pairwise ranking on graphs [29]. Such a theory, referred to as HodgeRank, was introduced by [61], [59] to multimedia QoE assessment. Roughly speaking, it says that all paired comparison data Y on graph G admits the following orthogonal decomposition:

$$\textit{aggregate paired comparisons} =$$

$$\text{global ranking} \oplus \text{harmonic cyclic} \oplus \text{triangular cyclic}.$$

In particular, the latter two subspaces, harmonic and triangular cyclic rankings, are both called cyclic ranking here (i.e., subspace $\ker(X^T)$).

Note that in (7), the unitary matrix U_2^T is an orthogonal projection onto the subspace of cyclic ranking. Therefore, it enables the following interpretation of outlier detection LASSO via Hodge Decomposition. The outlier γ in (7) is a *sparse approximation of the projection of paired comparison data onto cyclic ranking subspace*. This leads us to an extension of outlier detection by TSR in complete case to incomplete settings.

3.2.2 Parameter Tuning

A crucial question here is how to choose λ which is equivalent to estimate the variance of ε_{ij}^α properly. For this purpose, Huber [28] proposes the concomitant scale estimation, which jointly estimates s and λ via the following way:

$$\min_{\sum_{i\in V}\theta_i=0,\sigma} \sum_{i,j,\alpha} \rho_M\left(\frac{\theta_i - \theta_j - Y_{ij}^\alpha}{\sigma}\right)\sigma + m\sigma, \tag{10}$$

where m is the total number of paired comparisons. Note that $M\sigma$ plays the same role of λ in (5), since for fixed σ, minimization problem (10) is equivalent to minimize (5) with $\lambda = M\sigma$. In practice, [28] suggests to fix $M = 1.35$ in order to be robust as much as possible and do not lose much statistical efficiency for normally distributed data. Problem (10) becomes a convex optimization problem jointly in θ and σ, hence can be solved efficiently. In LASSO's formulation, Huber's concomitant scale estimation becomes scaled-lasso whose consistency is proved in [51].

However, in our applications the concomitant scale estimation (10) only works when outliers are sparse enough. Moreover, cross-validation to find optimal λ, turns out to be highly unstable here. Since every sample is associated with an outlier variable, leaving out samples thus loses all information about the associated outlier variables.

Here we suggest a new cross-validation scheme based on random projections. Note that U_2 is a projection onto the subspace $\ker(X^T)$, hence one can exploit subsets of random projections as training and validation sets, respectively. Each random projection will contain information of all the sample and outliers generically. Thanks to the exploitation of Erdös-Rényi random graphs in crowdsoucring experiments [61], [59], positions of outliers can be consistently identified with such a random projection based cross-validation.

In practice, although cross-validation works for sparse and large enough outliers, we find it might fail when outliers become dense and small in magnitudes. However, when cross-validation fails, we still find it more informative by looking at the regularization paths of (7) directly. The order that variables γ_{ij}^α become nonzero when regularization parameter λ changes from ∞ to small, can faithfully identify the tendency that a measurement Y_{ij}^α is contaminated by outliers, even when cross-validation fails. Therefore, we suggest to use regularization paths to inspect the outliers in applications.

Prior knowledge can also be used to tune the regularization parameter. For example, if one would like to drop a certain percentage of outliers, say 5%, then the top 5% variables appeared on regularization paths can be regarded as outliers and dropped. Moreover, the deviation magnitudes sometimes can be used to determine outliers. For example in dichotomous choice, we can just set $\lambda = 1$. If $\theta_i - \theta_j > 0$, and $Y_{ij}^\alpha = -1$ so the residual $|\gamma_{ij}^\alpha| = |\theta_i - \theta_j - Y_{ij}^\alpha| > 1$, then this comparison is easily to be picked out. On the other hand, if $Y_{ij}^\alpha = 1$, $|\gamma_{ij}^\alpha| > 1$ iff $\theta_i - \theta_j > 2$, which is reasonable to be selected as an outlier.

3.2.3 HLASSO Algorithm

Based on these development, we have the the following Robust Ranking Algorithm 1 called HLASSO here.

However, HLASSO suffers the following issues.

- Bias: HLASSO gives a biased estimation [20], $\hat{\gamma}$ and $\hat{\theta}$.
- Scalability: (7) is prohibitive with large number of samples and ranking items.

Algorithm 1: Outlier Detection and Robust Ranking, denoted by HLASSO.

1 **Initialization:** Compute the projection matrix U_2 via the SVD of X or (9);
2 **Solve the outlier detection LASSO** (7);
3 **Tuning parameter**. Determine an optimal λ^* by Huber's concomitant scale estimation (scaled-LASSO), or random projection based cross validation;
4 **Rule out outlier effect and perform least squares in** (8) **to obtain the score estimation** $\hat{\theta}$.

To remove bias, after correctly identifying the outliers, one can drop those comparisons contaminated by outliers and use the least squares estimation to achieve an unbiased estimation.

3.3 Scalable Algorithm: Linearized Bregman Iteration

Here we introduce some new algorithms inspired by certain ordinary differential equations (ODEs) leading to unbiased estimators [36]. The new algorithms are discretization of such ODEs which are easy for parallel implementation and scalable.

Consider the ODE

$$\frac{1}{\kappa}\dot{\theta} = \nabla_\theta \|Y - X\theta - \gamma\|^2 \tag{11a}$$

$$\dot{p} + \frac{1}{\kappa}\dot{\gamma} = \nabla_\gamma \|Y - X\theta - \gamma\|^2 \tag{11b}$$

$$p \in \partial\|\gamma\|_1. \tag{11c}$$

As the damping paramter $\kappa \to \infty$, we have

$$0 = \nabla_\theta \|Y - X\theta - \gamma\|^2 \tag{12a}$$

$$\dot{p} = \nabla_\gamma \|Y - X\theta - \gamma\|^2 \tag{12b}$$

$$p \in \partial\|\gamma\|_1. \tag{12c}$$

When sign-consistency is reached at certain τ, i.e., $p \in \partial\|\gamma^*\|_1$, then $\dot{p}_S(\tau) = 0$ ($S = \mathrm{supp}(\gamma^*)$) and we have

$$\begin{bmatrix} X^TX & X_S^T \\ X_S & I \end{bmatrix} \begin{bmatrix} \hat{\theta}(\tau) \\ \hat{\gamma}_S(\tau) \end{bmatrix} = \begin{bmatrix} X^TX & X_S^T \\ X_S & I \end{bmatrix} \begin{bmatrix} \theta^* \\ \gamma_S^* + \varepsilon \end{bmatrix}$$

which implies the optimal estimator is $\hat{\gamma}_S(\tau) = \gamma_S^* + \varepsilon$ which is unbiased and $\hat{\theta}(\tau)$ is the subset least square solution after removing outliers.

Linearized Bregman Iteration (LBI) Algorithm 2 is a forward Euler discretization of (11) with step size $\triangle t$ and $z^k = p^k + \frac{1}{\kappa}\gamma^k$.

Remark. The parameter $h = \kappa \cdot \triangle t$ is the step size of gradient decent of θ. So h should not be too large to make the algorithm converge. In fact necessarily $h\|XX^T + I\| \le h(\|XX^T\| + 1) < 2$ in Section 4.

Remark. The parameter κ is the damping factor of dynamic of γ and θ. As $\kappa \to \infty$ and $\triangle t \to 0$, the algorithm will converge to dynamics (12) which finds unbiased estimators when sign consistency is reached.

Remark. As we shall see in the next section, $t^k = k\triangle t$ plays a similar role as $1/\lambda$ in (6) to control the sparsity of γ. Sparsity is large as $k = 0$ from the empty set, and decreases with possible oscillations as iteration goes. Early stopping regularization is thus required to avoid overfitting. Similar ways of parameter tuning as Huber-LASSO can be applied here to find an early stopping rule $\tau = k^*\triangle t$.

Moreover, one can change the update of θ^k from gradient decent in (13a) to exact solution $\theta^k = (X^TX)^\dagger X(Y - \gamma^k)$, which gives Algorithm 3.

Algorithm 2: LBI in correspondence to (6)

1 **Initialization:** Given parameter κ and $\triangle t$, define $h = \kappa\triangle t$, $k = 0, z^0 = 0, \gamma^0 = 0$ and $\theta^0 = (X^TX)^{-1}XY$.
2 **Iteration:**

$$z^{k+1} = z^k + (Y - X\theta^k - \gamma^k)\triangle t. \tag{13a}$$

$$\gamma^{k+1} = \kappa\,\mathrm{shrink}(z^k). \tag{13b}$$

$$\theta^{k+1} = \theta^k + h\,X^T(Y - X\theta^k - \gamma^k). \tag{13c}$$

Stopping: exit when stopping rules are met.

Algorithm 3: LBI in correspondence to (7)

1 **Initialization:** Given parameter $\kappa, \triangle t$, define $k = 0, z^0 = 0, \gamma^0 = 0$.
2 **Iteration:**

$$z^{k+1} = z^k + (I - X(X^TX)^\dagger X^T)(Y - \gamma^k)\triangle t. \tag{14a}$$

$$\gamma^{k+1} = \kappa\,\mathrm{shrink}(z^k), \tag{14b}$$

Stopping: exit when stopping rules are met.

Note that $I - X(X^TX)^\dagger X^T$ is the projection matrix $U_2U_2^T$ which involves sparse matrix X and is thus more efficient than finding U_2 in large scale problems.

4 Statistical Consistency of Outlier Detection

In this part, we establish the statistical theory for outlier detection by HLASSO and LBI, respectively. As we shall see, the solution path of LBI shares almost the same good properties as that of LASSO, i.e., outlier detection consistency and l_2-error bounds of minimax optimal rates. They both consistently identify locations of outliers under nearly the same conditions. Such conditions, roughly speaking, require that the matrix U_2 satisfies an incoherence (or irrepresentable) condition and the sparse outliers have large enough magnitudes. However as the limit dynamics of LBI (12) is unbiased, LBI may estimate outlier magnitudes with less bias than HLASSO. Another distinction lies in that LBI exploits early stopping regularization while HLASSO chooses a regularization parameter λ.

Let $S = \mathrm{supp}(\gamma^*)$ and $\hat{S} = \mathrm{supp}(\hat{\gamma})$ where $\mathrm{supp}(x) = \{i : x_i \neq 0\}$, $\tilde{y} = U_2^T y, \Psi = U_2^T$. $\Psi^T\Psi : l^2(E) \to l^2(E)$ is thus an orthogonal projection of $x \in l^2(E)$ to the kernel $\ker(\mathrm{X^T})$. Recall that the number of alternatives

$n = |V|$ and the number of paired comparisons $m = |E|$. Denote the column vectors of Ψ with index in S (S^c) by Ψ_S (Ψ_{S^c}) and the number of rows in Ψ by l ($l = m - n + 1$). Let

$$\mu_\Psi := \max_{j \in S^c} \frac{1}{l} \|\Psi_j\|_2^2.$$

Now we have

$$\tilde{y} = \Psi\gamma^* + \tilde{\varepsilon} = \Psi_S\gamma_S^* + \Psi\varepsilon,$$

where

$$\mathrm{var}(\tilde{\varepsilon}) = \mathbb{E}[\varepsilon\varepsilon^{\mathrm{T}}] = \sigma^2 \mathrm{I}.$$

The following assumptions are for both HLASSO and LBI.

- (C1: Restricted Eigenvalue)

$$\Lambda_{\min}\left(\frac{1}{l}\Psi_S^T\Psi_S\right) = C_{\min} > 0.$$

- (C2: Irrepresentability) For some constant $\eta \in (0, 1]$,

$$\|\Psi_{S^c}^T\Psi_S(\Psi_S^T\Psi_S)^{-1}\|_\infty \le 1 - \eta.$$

The irrepresentable condition is easy to satisfy for large connected Erdös-Rényi random graphs, since Ψ tends to be an orthogonal matrix as $n \to \infty$ and $n/m \ll n/(n \log n) \to 0$.

Theorem 1 (Consistency of HLASSO): Let

$$\lambda \ge \frac{2\sigma\sqrt{\mu_\Psi}}{\eta}\sqrt{l \log m}.$$

Then with probability greater than

$$1 - 2m \exp\left\{-\frac{\lambda^2\eta^2}{2l\sigma^2\mu_\Psi}\right\} \ge 1 - 2m^{-1},$$

(7) has a unique solution $\hat{\gamma}_\lambda$ satisfying:

- If condition C1 and C2 hold, there are no false positive outliers, i.e., $\hat{S} \subseteq S$; and $\|\hat{\gamma}_S - \gamma_S^\star\|_\infty \le \frac{\lambda}{l} h(\eta, \Psi, \gamma^*)$, where

$$h(\eta, \Psi, \gamma^*) = \frac{\eta}{\sqrt{C_{\min}\mu_\Psi}} + \left\|\left(\frac{1}{l}\Psi_S^T\Psi_S\right)^{-1}\right\|_\infty.$$

  On the contrary if condition C2 fails, then $\mathbf{Prob}(\hat{S} \subseteq S) < 1/2$.
- If additionally assume (C3: Large Outlier) $\gamma_{min} := \min_{i \in S} |\gamma_i^*| > \frac{\lambda}{l} h(\eta, \Psi, \gamma^*)$, there will be no false positive and negative outliers, i.e., $\hat{S} = S(\gamma^\star)$ ($\mathrm{sign}(\hat{\gamma}) = \mathrm{sign}(\gamma^*)$). On the contrary, if condition C3 fails, then $\mathbf{Prob}(\mathrm{sign}(\hat{\gamma}) = \mathrm{sign}(\gamma^*)) < 1/2$.

Remark Condition C1 is necessary for the uniqueness of a sparse outlier γ^* whose support is contained in S. C2 and C3 are sufficient to ensure no-false-positive outliers and no-false-negative outliers, respectively. They are also necessary above.

Remark From the uniform bound one can reach

$$\|\hat{\gamma}_S - \gamma_S^*\|_2 \le \frac{\sqrt{s}\lambda}{l} h(\eta, \Psi, \gamma^*) = O(\sqrt{\frac{s \log m}{l}}), \quad s = |S|$$

which is the minimax-optimal rate.

Theorem 2 (Consistency of LBI): Given C1 and C2, let $h = \kappa\triangle t$, $t^k = k\triangle t$, $B = \gamma_{max} + 2\sigma\sqrt{\frac{\log m}{C_{min} l}} + \frac{\|\Psi\gamma\|_2 + 2s\sqrt{\log l}}{l\sqrt{C_{min}}}$, and

$$\bar{\tau} := \frac{(1 - B/\kappa\eta)\eta}{2\sigma\sqrt{\mu_\Psi}}\sqrt{\frac{1}{l \log m}}.$$

Assume κ is big enough to satisfy $B \le \kappa\eta$, and step size $\triangle t$ is small s.t. $h\|\Psi_S\Psi_S^T\| < 2$. Then with probability at least $1 - \frac{1}{m\sqrt{\log m}} - \frac{2}{n\sqrt{\log n}}$, Algorithm 3 has paths satisfying:

- **(No-false-positive)** For all k such that $t^k \le \bar{\tau}$, the path has no-false-positive, i.e., $\mathrm{supp}(\gamma^k) \subseteq S$;
- **(Sign-consistency)** Moreover, if the smallest magnitude γ_{min} is strong enough and κ is big enough to ensure

$$\gamma_{\min} \ge \frac{4\sigma}{C_{min}^{1/2}}\sqrt{\frac{\log m}{l}},$$

$$\bar{\tau} \ge \frac{8 + 4\log s}{\tilde{C}_{min}\gamma_{min}} + \frac{1}{\kappa\tilde{C}_{min}}\log(\frac{3\|\gamma\|_2}{\gamma_{\min}}) + 3\triangle t,$$

  where $\tilde{C}_{min} = C_{min} l(1 - h\|\Psi_S\Psi_S^T\|/2)$, then for $k^* = \lfloor \bar{\tau}/(\triangle t) \rfloor$, $\mathrm{sign}(\gamma^{k^*}) = \mathrm{sign}(\gamma)$.
- **(l_2-bound)** For some constant κ and C large enough such that

$$\bar{\tau} \ge \frac{1}{2\kappa\tilde{C}_{min}}(1 + \log\frac{l\|\gamma\|_2^2 + 4\sigma^2 s \log m/C_{min}}{C^2 s \log m}) \ldots$$
$$\ldots + \frac{4}{C\tilde{C}_{min}}\sqrt{\frac{l}{\log m}} + 2\triangle t,$$

  there is a k^*, $t^{k^*} \le \bar{\tau}$, such that

$$\|\gamma^{k^*} - \gamma\|_2 \le (C + \frac{2\sigma}{C_{min}^{1/2}})\sqrt{\frac{s \log m}{l}}.$$

Remark The theorems show that t^k in Algorithm 3 plays the same role of $1/\lambda$ in (7),

$$\bar{\tau}\lambda = (1 - B/\kappa\eta) \to 1, \text{ as } \kappa \to \infty.$$

Therefore, early stopping in LBI plays a role of regularization as tuning λ in LASSO.

5 EXPERIMENTS

In this section, six examples are exhibited with both simulated and real-world data to illustrate the validity of the analysis above and applications of the methodology proposed. The first two examples are with simulated data while the latter four exploit real-world data in QoE evaluation and sports. Note that one dataset in QoE is collected by crowdsourcing.

TABLE 1: AUC over (SN,OP) for simulated data via LASSO, 20 times repeat.

AUC (sd)	OP=5%	OP=10%	OP=15%	OP=20%	OP=25%	OP=30%	OP=35%	OP=40%	OP=45%	OP=50%
SN=1000	0.999(0)	0.999(0.001)	0.998(0.001)	0.996(0.003)	0.992(0.005)	0.983(0.010)	0.962(0.016)	0.903(0.038)	0.782(0.050)	0.503(0.065)
SN=2000	0.999(0)	0.999(0)	0.999(0)	0.998(0.001)	0.997(0.001)	0.992(0.004)	0.986(0.007)	0.956(0.019)	0.849(0.052)	0.493(0.086)
SN=3000	0.999(0)	0.999(0)	0.999(0)	0.999(0)	0.998(0)	0.996(0.002)	0.990(0.004)	0.971(0.013)	0.885(0.032)	0.479(0.058)
SN=4000	0.999(0)	0.999(0)	0.999(0)	0.999(0)	0.999(0)	0.997(0.001)	0.994(0.002)	0.980(0.008)	0.903(0.028)	0.519(0.055)
SN=5000	0.999(0)	0.999(0)	0.999(0)	0.999(0)	0.999(0)	0.998(0.001)	0.994(0.002)	0.984(0.009)	0.933(0.022)	0.501(0.066)

TABLE 2: AUC over (SN,OP) for simulated data via LBI, 20 times repeat.

AUC (sd)	OP=5%	OP=10%	OP=15%	OP=20%	OP=25%	OP=30%	OP=35%	OP=40%	OP=45%	OP=50%
SN=1000	0.999(0.001)	0.999(0.001)	0.998(0.002)	0.997(0.003)	0.992(0.005)	0.981(0.009)	0.961(0.019)	0.909(0.032)	0.795(0.069)	0.497(0.069)
SN=2000	1.000(0)	0.999(0)	0.999(0.001)	0.999(0.001)	0.998(0.002)	0.993(0.005)	0.984(0.008)	0.957(0.017)	0.848(0.039)	0.476(0.087)
SN=3000	1.000(0)	1.000(0)	0.999(0)	0.999(0)	0.999(0.001)	0.996(0.004)	0.990(0.006)	0.973(0.014)	0.902(0.037)	0.521(0.085)
SN=4000	1.000(0)	1.000(0)	1.000(0)	0.999(0)	0.999(0.001)	0.998(0.002)	0.993(0.004)	0.976(0.001)	0.919(0.027)	0.487(0.061)
SN=5000	1.000(0)	1.000(0)	1.000(0)	0.999(0)	0.999(0.001)	0.998(0.001)	0.996(0.004)	0.983(0.007)	0.929(0.029)	0.502(0.064)

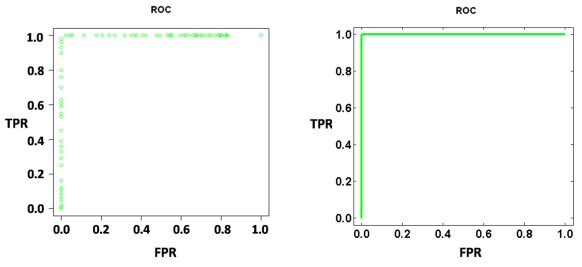

(a) LASSO (b) LBI

Fig. 1: ROC curve of $(2000, 5\%)$ of simulated data.

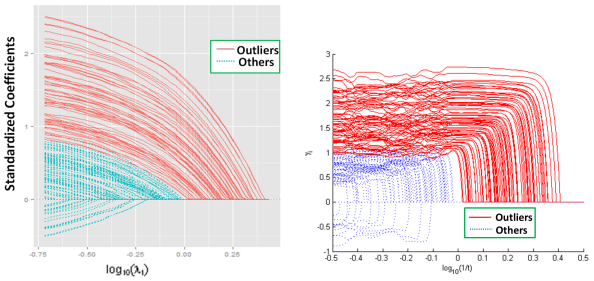

(a) LASSO (b) LBI

Fig. 2: The regularization paths of $(2000, 5\%)$ of LASSO vs. LBI. The true outliers (plotted in red color) mostly lie outside the majority of paths.

5.1 Simulated Study

5.1.1 *Experiment I: Synthetic pairwise data*

In this experiment, we first create a random total order on n candidates V as the ground-truth and add paired comparison edges $(i, j) \in E$ to graph $G = (V, E)$ randomly, with the preference direction following the ground-truth order. To create sparse outliers, a random subset of E is reversed in preference direction. In this way, we simulate a paired comparison graph, possibly incomplete and imbalanced, with outliers.

Here we choose $n = |V| = 16$, which is consistent with the first two real-world datasets. For convenience, denote the total number of paired comparisons by SN (Sample Number), the number of outliers by ON (Outlier Number), and the outlier percentage by OP = ON/SN. The following will show the proposed LBI could exhibit comparable performance with LASSO for outlier detection.

First, for each pair of (SN,OP), we compute the regularization path $\hat{\gamma}^\lambda$ of LASSO by varying regularization parameter λ from ∞ to 0, which is solved by R-package `quadrupen` [24]. The order in which $\hat{\gamma}^\lambda_{ij}$ becomes nonzero gives a ranking of the edges according to their tendency to be outliers. Since we have the ground-truth outliers, the ROC curve can be plotted by thresholding the regularization parameter λ at different levels which creates different true positive rates (TPR) and false positive rates (FPR). For example, when SN = 2000 and OP = 5%, the ROC curve can be seen in Fig. 1(a). With different choices of SN and OP, Area Under the Curve (AUC) are computed with standard deviations over 20 runs and shown in Table 1 to measure the performance of LASSO in outlier detection. Moreover, comparable results returned by LBI can be found in Fig. 1(b) and Table 2. It can be seen that when samples are large and outliers are sparse, the AUC of both of these two methods are close to 1. This implies that both LASSO and LBI can provide an accurate estimation of outliers (indicated by a small FPR with large TPR). Fig. 2(a), 2(b) illustrate the regularization path examples of LASSO and LBI.

We note that when OP = 50%, i.e., half of the edges are reverted by outliers, Table 1 and 2 both show a rapid decrease of AUC to about 0.5, which is the performance of random guess. This is as expected, since when more than half of the edges are perturbed, it is impossible to distinguish the signal from noise by any method. A phase transition can be observed in these two tables, that AUC rapidly increases to 1 as long as OP drops below 50% and SN increases.

The simulated example mentioned above tells us that LBI could exhibit similar performance with LASSO in most cases when sample numbers are not large. But when the sample number grows to be large, LASSO paths will be too expensive to compute while LBI still scales up. The following experiment provides

Fig. 3: Results of L2/LBI for image reconstruction with mean squared error.

such an example.

5.1.2 Experiment II: Image Reconstruction

In some scenarios like image reconstruction, there is a large number of samples (paired comparisons between pixels in images) and every sample contributes to an outlier variable, which makes LASSO difficult to detect outliers effectively. However LBI could provide us a simple yet scalable outlier detection algorithm for large-scale data analysis.

Here we use an simulation example of image reconstruction from [66]. First we use an image as the ground-truth, with an intensity range of $[0, 1]$ over 181×162 pixels. Local comparisons are obtained as intensity differences between pixels within a 5×5 neighborhood, added with Gaussian noise of $\sigma = 0.05$. Furthermore 10% of these measurements are added with random outliers of ± 0.5. So there are $n = 29,322$ nodes and $m = 346,737$ pairwise comparisons. In this example, none of the LASSO packages in this paper can deal with this example; in contrast, LBI takes the advantage of sparsity of X and works well. Fig. 3 shows the results marked by their mean squared errors with respect to the original image where LBI exhibits a significantly smaller error than the least squares (L2).

5.2 Real-world Datasets

As there is no ground-truth for outliers in real-world data, one can not exploit ROC and AUC as in simulated data to evaluate outlier detection performance here. In this subsection, we inspect the top $p\%$ pairs returned by LASSO/LBI and compare them with the whole data to see if they are reasonably good outliers. Besides, to see the effect of outliers on global ranking scores, we will further show the outcomes of four ranking algorithms, namely L2 (HodgeRank), HLASSO which is biased, LBI which is less biased, and LASSO+L2, a debiased HLASSO which first adopts LASSO for outlier detection followed by subset least square (L2) after dropping outlier contaminated examples. Numerical experimental results fit our theory nicely. Besides, we denote LBI algorithms by LBI $(\kappa, \triangle t)$ for parameter choices.

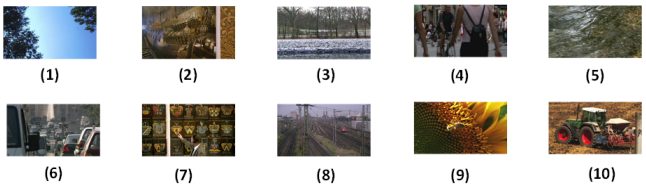

Fig. 4: Reference videos in LIVE database.

5.2.1 PC-VQA Dataset

The first dataset, PC-VQA, collected by [61], contains $38,400$ paired comparisons of the LIVE dataset [2] (Fig. 4) from 209 random observers. An attractive property of this dataset is that the paired comparison data is complete and balanced. As LIVE includes 10 different reference videos and 15 distorted versions of each reference, for a total of 160 videos, the complete comparisons of this video database requires $10 \times \binom{16}{2} = 1200$ comparisons. Therefore, $38,400$ comparisons correspond to 32 complete rounds.

For simplicity, we randomly take reference 1 as an illustrative example (other reference videos exhibit similar results). Outliers detected by both methods are shown in the paired comparison matrix in Table 3. This matrix is constructed as follows (Table 4 is constructed in the same way). For each video pair $\{i, j\}$, let n_{ij} be the number of comparisons, for which a_{ij} raters agree that the quality of i is better than j (a_{ji} carries the opposite meaning). So $a_{ij} + a_{ji} = n_{ij}$ if no tie occurs. In the PC-VQA dataset, $n_{ij} \equiv 32$ for all videos. The order of the video ID in Table 3 is arranged from high to low according to the global ranking score calculated by the least squares method (3). It is interesting to see that the outliers picked out are mainly distributed in the lower left corner of this matrix, which implies that the outliers are those preference orders with a large deviation from the global ranking scores by L2. In addition, the earlier a pair is detected as an outlier, the closer it will be to the lower left corner and the larger such a deviation is. Moreover, Fig. 5 further confirms this phenomenon. Here, all the top 5% outliers are reversed preference arrows pointing from lower quality to higher quality videos. More importantly, it is easy to see that outliers returned by these two approaches are almost the same with a few exceptions shown by open/filled blue circles in Table 3 and red/blue lines in Fig. 5. The reason why the difference occurs lies in the solution accuracy of LASSO, in which more than one pair corresponding to the same λ may jump out together at the same time to become outliers. From this viewpoint, the detection difference between LBI and LASSO frequently happens on the last few pairs.

Table 5(a) shows the outcomes of the four ranking algorithms mentioned above. It is easy to see that removal of the top 5% outliers in both LASSO+L2 and LBI $(50, 1/25000)$ changes the orders of some compet-

TABLE 3: Paired comparison matrixes of reference 1 in PC-VQA dataset. Red pairs for top 5% outliers obtained by both LASSO vs. LBI. Open blue circles are those obtained by LASSO but not LBI, while filled blue circles are obtained by LBI but not LASSO.

Video ID	**1**	**9**	**10**	**13**	**7**	**8**	**11**	**14**	**15**	**3**	**12**	**4**	**16**	**5**	**6**	**2**
1	0	22	29	30	30	29	29	29	30	28	29	32	32	31	32	31
9	10	0	22	20	14	23	23	25	29	29	32	30	29	30	29	31
10	3	10	0	22	11	21	29	23	31	27	31	30	32	30	32	31
13	2	12	10	0	18	22	23	27	31	28	29	29	29	25	27	28
7	❷	18	21	14	0	21	14	16	28	23	31	25	19	27	26	28
8	3	9	11	10	11	0	25	14	28	25	29	27	24	25	28	32
11	3	9	3	9	18	7	0	22	27	26	26	30	30	27	27	31
14	3	7	9	5	16	18	10	0	28	27	18	29	29	26	28	29
15	2	3	1	1	4	4	5	4	0	25	20	22	26	25	29	24
3	4	3	5	4	9	7	6	5	7	0	11	15	26	24	29	28
12	3	0	1	3	1	3	6	14	12	21	0	16	20	24	26	26
4	0	2	2	3	7	5	2	3	10	17	16	0	15	26	27	30
16	0	3	0	3	13	8	2	3	6	6	12	17	0	22	24	28
5	1	2	2	7	5	7	5	6	7	8	8	6	10	0	26	27
6	0	3	0	5	6	4	5	4	3	3	6	5	8	6	0	21
2	1	1	1	4	4	0	1	3	8	4	6	②	4	5	11	0

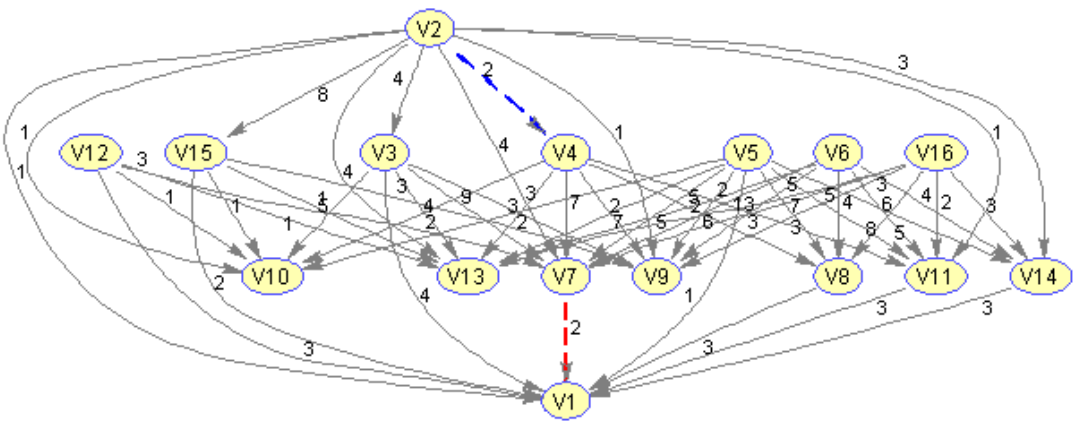

Fig. 5: Top 5% outliers for reference 1 in PC-VQA dataset. The integer on each curve represents a_{ij} defined in subsection 5.2.1. The pair with red line indicates LBI detects it as an outlier but LASSO does not, while blue line means LASSO treats it as an outlier but LBI does not.

itive videos, such as V3 and V12. More importantly, both changes are in the same way, which indicates HLASSO is more biased than them and the effect of outliers is mainly within the highly competitive groups.

5.2.2 PC-IQA Dataset

Additionally, to test the detection ability on incomplete and imbalanced data, PC-IQA dataset is taken into consideration. This dataset contains 15 reference images and 15 distorted versions of each reference, for a total of 240 images which come from two publicly available datasets, LIVE [2] and IVC [1] (Fig. 6). Totally, 186 observers, each of whom performs a varied number of comparisons via Internet, provide $23,097$ paired comparisons for crowdsourced subjective image quality assessment.

Table 4 and Fig. 7 show the experimental results on a randomly selected reference (image 10 in Fig. 6). Similar observations as above can be made and we note that outliers distributed on this dataset are much sparser than PC-VQA, shown by many zeros in the lower left corner of Table 4. The outcomes of four ranking algorithms with the top 5% outliers are shown in Table 5(b). Based on 5% outliers detection, HLASSO, LBI $(50, 1/25000)$, and LASSO+L2 all differ with L2 in that image ID = 3 (`fruit_flou_f3.bmp` in IVC [1] database) is better than image ID = 14 (`fruit_lar_r1.bmp`). Such a preference is in agreement with the pairwise majority voting of 9:6 votes

TABLE 4: Paired comparison matrixes of reference 10 in PC-IQA dataset. Red pairs, open blue circles, and filled blue circles carry the same meanings with Table 3.

Image ID	1	6	9	12	10	2	16	7	15	11	8	13	14	3	4	5
1	0	11	10	12	11	20	11	15	13	14	16	15	14	17	14	13
6	3	0	5	10	8	11	11	12	10	10	12	13	12	11	14	16
9	3	7	0	5	7	6	3	10	4	5	8	6	5	11	14	17
12	3	2	3	0	6	9	13	7	8	5	8	13	13	13	16	17
10	5	4	0	2	0	7	2	5	6	7	9	5	6	12	17	19
2	0	3	5	4	4	0	8	9	9	13	6	11	12	12	13	13
16	3	1	1	2	2	4	0	6	16	8	7	16	16	15	20	14
7	0	2	1	1	4	2	4	0	7	5	12	8	9	13	17	16
15	0	4	1	4	1	❹	3	2	0	8	7	12	16	16	16	14
11	0	0	0	0	0	0	3	4	1	0	9	2	6	11	14	17
8	0	0	0	0	0	4	0	0	0	0	0	5	8	10	15	17
13	0	0	0	0	0	0	0	0	4	2	1	0	12	13	15	16
14	0	0	1	0	0	0	1	0	0	2	1	2	0	6	12	10
3	0	0	0	0	0	0	0	0	0	0	0	0	9	0	10	10
4	0	0	0	0	0	0	0	0	0	2	0	2	4	1	0	9
5	0	0	0	0	0	0	0	0	0	1	0	0	⑤	①	5	0

Fig. 6: Reference images in LIVE and IVC databases. (The first six are from LIVE and the remaining nine are from IVC.)

TABLE 5: Comparison of different rankings (5% outliers are considered). Four ranking methods are compared with the integer representing the ranking position and the number in parentheses representing the global ranking score returned by the corresponding algorithm.

(a) Reference 1 in PC-VQA dataset

ID	L2	HLASSO	LBI	LASSO+L2
1	1 (0.7930)	1 (0.8103)	1 (0.8648)	1 (0.8688)
9	2 (0.5312)	2 (0.5478)	2 (0.5987)	2 (0.5996)
10	3 (0.4805)	3 (0.4892)	3 (0.5253)	3 (0.5253)
13	4 (0.3906)	4 (0.4155)	4 (0.5059)	4 (0.5100)
7	5 (0.2852)	5 (0.3104)	5 (0.4266)	5 (0.4570)
8	6 (0.2383)	6 (0.2501)	6 (0.3059)	6 (0.3156)
11	7 (0.2148)	7 (0.2234)	7 (0.2550)	7 (0.2601)
14	8 (0.1641)	8 (0.1719)	8 (0.2061)	8 (0.2125)
15	9 (-0.1758)	9 (-0.1785)	9 (-0.1817)	9 (-0.1749)
3	10 (-0.2227)	10 (-0.2361)	11 (-0.2918)	11 (-0.3017)
12	11 (-0.2500)	11 (-0.2562)	10 (-0.2781)	10 (-0.2800)
4	12 (-0.2930)	12 (-0.3015)	12 (-0.3498)	12 (-0.3608)
16	13 (-0.3633)	13 (-0.3788)	13 (-0.4673)	13 (-0.4812)
5	14 (-0.4414)	14 (-0.4651)	14 (-0.5703)	14 (-0.5760)
6	15 (-0.6289)	15 (-0.6570)	15 (-0.7398)	15 (-0.7412)
2	16 (-0.7227)	16 (-0.7455)	16 (-0.8086)	16 (-0.8332)

(b) Reference 10 in PC-IQA dataset

ID	L2	HLASSO	LBI	LASSO+L2
1	1 (0.8001)	1 (0.8144)	1 (0.8851)	1 (0.8876)
6	2 (0.6003)	2 (0.6143)	2 (0.6977)	2 (0.7034)
9	3 (0.5362)	3 (0.5484)	3 (0.5929)	3 (0.6048)
12	4 (0.4722)	4 (0.4752)	4 (0.4895)	4 (0.4886)
10	5 (0.3472)	5 (0.3368)	6 (0.2770)	6 (0.2698)
2	6 (0.3044)	6 (0.3105)	5 (0.3115)	5 (0.2859)
16	7 (0.2756)	7 (0.2757)	7 (0.2680)	7 (0.2677)
7	8 (0.1403)	8 (0.1374)	8 (0.1392)	8 (0.1398)
15	8 (0.0965)	9 (0.0865)	9 (0.0418)	9 (0.0540)
11	10 (-0.1609)	10 (-0.1563)	10 (-0.1739)	10 (-0.1815)
8	11 (-0.2541)	11 (-0.2620)	11 (-0.2803)	11 (-0.2813)
13	12 (-0.2964)	12 (-0.2958)	12 (-0.2929)	12 (-0.2927)
14	13 (-0.6215)	14 (-0.6799)	14 (-0.6478)	14 (-0.6478)
3	14 (-0.6315)	13 (-0.6316)	13 (-0.6246)	13 (-0.6246)
4	15 (-0.7822)	15 (-0.7889)	15 (-0.8102)	15 (-0.8098)
5	16 (-0.8262)	16 (-0.8287)	16 (-0.8339)	16 (-0.8639)

(Table 4). Therefore, the example shows that under sparse outliers L2 ranking may be less accurate.

Moreover, LASSO+L2 and LBI further suggest that image ID = 2 should be better than image ID = 10, in contrast to L2 and HLASSO algorithms. A further inspection of the dataset confirms that such a suggestion is reasonable. Fig. 8 shows the two images (ID = 2 and ID = 10) from the IVC [1] database. There is a blurring effect in image ID = 2 and a blocking effect in the background of ID = 10. In the dataset, 4 raters agree that the quality of ID = 2 is better than ID = 10, while 7 raters have the opposite opinion. Clearly both LASSO+L2 and LBI choose the preference of the minority, based on aggregate behavior over population after removal of some outliers. Why does this happen? In fact, when a participant compares the quality between ID = 2 and ID = 10, his preference depends on his attention — on the foreground or on the whole image. A rater with foreground attention might be disturbed by the blurring effect, leading to $10 \succ 2$. On the other hand, a rater with holistic attention may notice the blocking effect in the background, leading to $2 \succ 10$. Which criterion might be dominant? To explore this

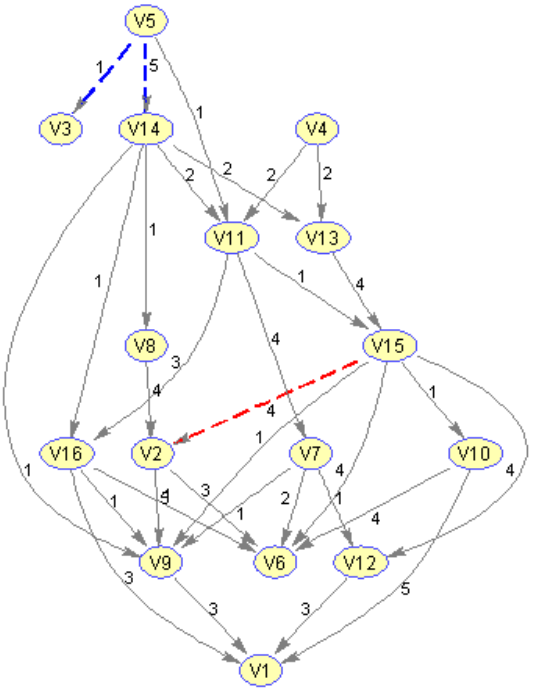

Fig. 7: Top 5% outliers for reference 10 in PC-IQA dataset. The integer on each curve and the red/blue lines carry the same meanings with those in Fig. 5.

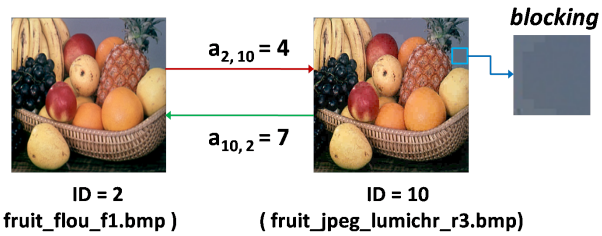

Fig. 8: Dissimilar judgments due to multi-criteria in paired comparisons among users. The image is undistinguishable due to its small size, so image names in IVC [1] database are printed here.

TABLE 6: Thirteen outliers as matches picked out in NBA 2010-2011 data, with final scores in games. These outliers share a common feature with a big final score difference.

Guest team	Score	Score	Host team
Hornets	100	59	Hawks
Cavaliers	57	112	Lakers
76ers	76	121	Bulls
76ers	117	83	Hawks
Hawks	83	115	Wizards
Nuggets	113	144	Pacers
Magic	107	78	Bulls
Kings	127	95	Timberwolves
Bobcats	75	108	Wizards
Raptors	100	138	Braves
Jazz	120	99	Thunder
Bucks	98	79	Lakers
Bulls	114	81	Hawks

question, we further collected more clean data (i.e., 20 more persons provide careful judgments in controlled lab conditions), among which a dominant percentage (80%) agrees with $2 \succ 10$, consistent with the LASSO+L2/LBI prediction after removal of outliers. This suggests that most observers assess the quality of an image from a global point of view. Another less stable way is to select a subset of clean data without outliers for validation. Such a result suggests that for those highly competitive or confused alternative pairs, a large number of samples are expected to find a good ranking in majority voting; on the other hand, by exploiting intermediate comparisons of good confidence with other alternatives, it is possible to achieve a reliable global ranking with a much smaller number of samples, such as what LASSO+L2/LBI does here.

5.2.3 NBA Dataset

The third example studies the NBA (National Basketball Association) 2010-2011 regular season games. The NBA has 30 teams and every year, each team plays 82 matches in the regular season. The results of the 1230 total matches from the 2010-2011 regular season were downloaded from NBA Dataset. Here we use the differences of game scores as paired comparison data and put equal weight on all the games. The resulting graph thus consists of 30 nodes with 1230 comparisons. It should be noted that there is head-advantage (home advantage) here to be captured by an additional intercept parameter in linear model (1). That is, it is more likely for a team to win when playing at home than away due to the support of fans.

A close inspection on regularization paths reveals several outliers, with top thirteen shown in Table 6 and it is interesting to see that outliers selected by LASSO and LBI are the same. Such outliers are unexpected as the strong team is beaten by the weak. For example, an outlier shows that Bucks beats Lakers by 98:79. However Lakers got 57wins/25loses in that season and was ranked 2nd in Western Conference, while Bucks got 35wins/47loses and was ranked 9th in Eastern Conference. This is definitely regarded as an unexpected result at that time.

To compare different ranking algorithms, Table 7 shows global ranking order and scores returned by four algorithms. It is easy to see that LBI $(5000, 1/500000)$ could approach the scores of LASSO+L2 successfully. More importantly, the larger the κ is, the closer LBI approaches LASSO+L2 which is unbiased.

5.2.4 Tennis Match Dataset

The data is provided by Braxton Osting and details on data collection can be found in [37]. The dataset consists of $4,074$ matches during October 9, 2010 to October 5, 2011, played between 218 players each of which played at least 27 matches. At the end of each tennis match, there is a winner and a loser; there are

TABLE 7: Comparison of different rankings on NBA data. Four ranking methods are compared with the integer representing the ranking position and the number in parenthsis representing the global ranking score returned by the corresponding algorithm. The last line shows the intercept estimator which shows the home advantage is almost a 3-point ball.

Team name	L2	HLASSO	LBI	LASSO+L2
Heat	1 (6.7560)	1 (6.7637)	1 (6.7833)	1 (6.7833)
Bulls	2 (6.5320)	2 (6.5043)	2 (6.1420)	2 (6.1388)
Lackers	3 (6.0082)	3 (5.9068)	3 (5.8865)	3 (5.8874)
Spurs	4 (5.8633)	4 (5.8574)	4 (5.8499)	4 (5.8499)
Magic	5 (4.9245)	5 (4.8737)	7 (4.5503)	7 (4.5504)
Celtics	6 (4.8252)	7 (4.8279)	6 (4.8269)	6 (4.8268)
Nuggets	7 (4.8055)	6 (4.8639)	5 (5.2033)	5 (5.2033)
Mavericks	8 (4.4076)	8 (4.4019)	8 (4.3865)	8 (4.3865)
Thunder	9 (3.8119)	9 (3.8139)	9 (4.1498)	9 (4.1499)
Grizzlies	10 (2.5455)	10 (2.5383)	10 (2.5268)	10 (2.5268)
Rockets	11 (2.3738)	11 (2.3683)	11 (2.3610)	11 (2.3610)
Blazers	12 (1.8453)	12 (1.8394)	12 (1.8319)	12 (1.8319)
Hornets	13 (1.2789)	13 (1.1143)	14 (0.7427)	14 (0.7425)
76ers	14 (1.0055)	14 (1.0235)	13 (1.0219)	13 (1.0219)
Knicks	15 (0.4828)	15 (0.4908)	16 (0.5105)	16 (0.5105)
Suns	16 (-0.4582)	16 (-0.4656)	17 (-0.4771)	17 (-0.4771)
Bucks	17 (-1.0148)	18 (-1.0104)	18 (-1.3329)	18 (-1.3337)
Hawks	18 (-1.0966)	17 (-0.7795)	15 (0.6490)	15 (0.6525)
Pacers	19 (-1.3747)	19 (-1.4295)	19 (-1.7608)	19 (-1.7608)
Jazz	20 (-1.4414)	20 (-1.4555)	20 (-1.8102)	20 (-1.8103)
Braves	21 (-2.004)	21 (-2.0307)	21 (-2.3888)	21 (-2.3888)
Clippers	22 (-2.7145)	22 (-2.7193)	22 (-2.7225)	22 (-2.7225)
Pistons	23 (-3.7816)	23 (-3.7729)	24 (-3.7494)	24 (-3.7494)
Bobcats	24 (-4.0779)	24 (-4.0209)	23 (-3.6624)	23 (-3.6624)
Kings	25 (-4.8029)	25 (-4.8722)	25 (-5.2311)	25 (-5.2310)
Timberwolves	26 (-5.9689)	26 (-5.9111)	26 (-5.5709)	26 (-5.5709)
Raptors	27 (-6.2753)	27 (-6.2509)	27 (-5.9090)	27 (-5.9090)
Nets	28 (-6.2810)	28 (-6.2721)	28 (-6.2448)	28 (-6.2448)
Wizards	29 (-7.2966)	29 (-7.419)	29 (-8.1102)	29 (-8.1104)
Cavaliers	30 (-8.8776)	30 (-8.7783)	30 (-8.4524)	30 (-8.4525)
intercept	3.1675	3.1652	3.1888	3.1900

TABLE 8: Top eight outliers in Tennis data. ATP ranking on Oct 10, 2011 is shown after player's name. All these outlier matches are featured with lower ranked players beating higher ranked players.

Winner	Loser
FARAH, Robert (COL)[209]	TURSUNOV, Dmitry (RUS)[41]
WARD, James (GBR)[152]	WAWRINKA, Stanislas (SUI)[19]
MANNARINO, Adrian (FRA)[89]	DEL POTRO, Juan Martin (ARG)[14]
RAMIREZ-HIDALGO, Ruben (ESP)[133]	CILIC, Marin (CRO)[22]
DAVYDENKO, Nikolay (RUS)[37]	NADAL, Rafael (ESP)[2]
BELLUCCI, Thomaz (BRA)[35]	MURRAY, Andy (GBR)[4]
MARTI, Javier (ESP)[188]	HARRISON, Ryan (USA)[79]
KAMKE, Tobias (GER)[96]	BERDYCH, Tomas (CZE)[7]

no ties in this data. Hence the paired comparison data is binary, $y_{ij} = -y_{ji} \in \{\pm 1\}$.

The top eight outliers returned by LASSO and LBI are also the same, as shown in Table 8. Different rankings returned by four algorithms are shown in Table 9 with LBI $(10000, 1/1000000)$. These outliers are all made up of by the events that high-ranked players are beaten by low-ranked players. For example, NADAL Rafael (ranked 3rd in all four) are beaten by DAVYDENKO Nikolay (ranked 37-40) in the fifth outlier appeared in LASSO regularization paths. Besides, similar to the NBA dataset, it is easy to see that LBI could also approach the scores of unbiased LASSO+L2 successfully, both of which are different to the biased HLASSO ranking.

6 CONCLUSIONS

In this paper, we propose a framework of robust ranking with pairwise comparison data on graphs, based on the principle of Huber's robust statistics. Outlier detection can be formulated as a LASSO optimization problem which looks for sparse approximations of cyclic ranking projection in Hodge decomposition. Simple and scalable algorithms are proposed with Linearized Bregman Iterations which are less biased than LASSO. Statistical consistency theory is established for both cases. Experimental studies are conducted with both simulated examples and real-world data. Our results suggest that Linearized Bregman Iteration is a promising computational tool for robust ranking with large scale crowdsourcing data.

TABLE 9: Comparison of different ranking methods on Tennis data. It shows the global ranking positions (scores) of top ten players and those involved in the eight outlier matches.

Player name (Country)	L2	HLASSO	LBI	LASSO+L2
DJOKOVIC, Novak (SRB)	1 (1.1978)	1 (1.1984)	1 (1.2072)	1 (1.2072)
FEDERER, Roger (SUI)	2 (1.1555)	2 (1.1563)	2 (1.1650)	2 (1.1650)
NADAL, Rafael (ESP)	3 (1.0912)	3 (1.0934)	3 (1.1230)	3 (1.1230)
MURRAY, Andy (GBR)	4 (0.9114)	4 (0.9125)	4 (0.9427)	4 (0.9427)
SODERLING, Robin (SWE)	5 (0.8608)	5 (0.8614)	6 (0.8692)	6 (0.8692)
DEL POTRO, Juan Martin (ARG)	6 (0.8298)	6 (0.8334)	5 (0.8704)	5 (0.8704)
FERRER, David (ESP)	7 (0.7799)	7 (0.7803)	7 (0.7851)	7 (0.7851)
TSONGA, Jo-Wilfried (FRA)	8 (0.7195)	8 (0.7198)	8 (0.7247)	8 (0.7247)
FISH, Mardy (USA)	9 (0.7034)	9 (0.7039)	9 (0.7107)	9 (0.7107)
MONFILS, Gael (FRA)	10 (0.6755)	10 (0.6761)	10 (0.6819)	10 (0.6819)
BERDYCH, Tomas (CZE)	11 (0.6386)	11 (0.6392)	11 (0.6655)	11 (0.6660)
...	...	...	...	...
CILIC, Marin (CRO)	19 (0.5242)	19 (0.5273)	15 (0.5612)	15 (0.5612)
WAWRINKA, Stanislas (SUI)	24 (0.4819)	23 (0.4868)	20 (0.5235)	20 (0.5236)
TURSUNOV, Dmitry (RUS)	34 (0.3527)	34 (0.3576)	32 (0.3916)	32 (0.3916)
DAVYDENKO, Nikolay (RUS)	37 (0.3238)	37 (0.3218)	40 (0.2932)	40 (0.2932)
BELLUCCI, Thomaz (BRA)	54 (0.2218)	54 (0.2210)	55 (0.1896)	55 (0.1897)
HARRISON, Ryan (USA)	68 (0.1037)	68 (0.1042)	62 (0.1331)	62 (0.1331)
MANNARINO, Adrian (FRA)	88 (0.0245)	91 (0.0209)	100 (-0.0145)	100 (-0.0145)
KAMKE, Tobias (GER)	102 (-0.0227)	102 (-0.0228)	110 (-0.0491)	110 (-0.0497)
RAMIREZ-HIDALGO, Ruben (ESP)	174 (-0.2735)	175 (-0.2771)	182 (-0.3179)	182 (-0.3179)
WARD, James (GBR)	196 (-0.3945)	199 (-0.4036)	205 (-0.4670)	205 (-0.4670)
FARAH, Robert (COL)	212 (-0.5379)	212 (-0.5458)	213 (-0.5989)	213 (-0.5990)
MARTI, Javier (ESP)	213 (-0.5743)	213 (-0.5758)	214 (-0.6371)	214 (-0.6371)

REFERENCES

[1] Subjective quality assessment irccyn/ivc database. http://www2.irccyn.ec-nantes.fr/ivcdb/, 2005.

[2] LIVE image & video quality assessment database. http://live.ece.utexas.edu/research/quality/, 2008.

[3] A. Agrawal, R. Raskar, S. K. Nayar, and Y. Li. Removing photography artifacts using gradient projection and flash-exposure sampling. *ACM Transactions on Graphics*, 24(3):828–835, 2005.

[4] A.-L. Barabasi and R. Albert. Emergence of scaling in random networks. *Science*, 286(5439):509–512, 1999.

[5] A. Beck and M. Teboulle. A fast iterative shrinkage-thresholding algorithm for linear inverse problems. *SIAM Journal on Imaging Sciences*, 2(1):183–202, 2009.

[6] S. Boyd and L. Vandenberghe. *Convex optimization*. Cambridge University Press, 2004.

[7] R. Bradley and M. Terry. Rank analysis of incomplete block designs, i. the method of paired comparisons. *Biometrika*, 39:324–345, 1952.

[8] S. Brin and L. Page. The anatomy of a large-scale hypertextual web search engine. *Computer networks and ISDN systems*, 30(1):107–117, 1998.

[9] K.-T. Chen, C.-C. Wu, Y.-C. Chang, and C.-L. Lei. A crowdsourceable QoE evaluation framework for multimedia content. pages 491–500. ACM Multimedia, 2009.

[10] C. Cortes, M. Mohri, and A. Rastogi. Magnitude-preserving ranking algorithms. In *International conference on Machine learning*, pages 169–176. ACM, 2007.

[11] H. David. *The method of paired comparisons*. 2nd Ed., Griffin's Statistical Monographs and Courses, 41. Oxford University Press, New York, NY, 1988.

[12] J. C. de Borda. Mémoire sur les élections au scrutin. 1781.

[13] M. de Condorcet. Éssai sur l'application de l'analyse à la probabilité des décisions rendues à la pluralité des voix (essay on the application of analysis to the probability of majority decisions). *Imprimerie Royale, Paris*, 1785.

[14] D. L. Donoho. De-noising by soft-thresholding. *IEEE Transactions on Information Theory*, 41(3):613–627, 1995.

[15] C. Dwork, R. Kumar, M. Naor, and D. Sivakumar. Rank aggregation methods for the web. In *International Conference on World Wide Web*, pages 613–622, 2001.

[16] A. Eichhorn, P. Ni, and R. Eg. Randomised pair comparison: an economic and robust method for audiovisual quality assessment. pages 63–68. ACM Workshop on Network and Operating Systems Support for Digital Audio and Video, 2010.

[17] N. El Karoui, D. Bean, P. J. Bickel, C. Lim, and B. Yu. On robust regression with high-dimensional predictors. *Proceedings of the National Academy of Sciences*, 110(36):14557–14562, 2013.

[18] P. Erdos and A. Renyi. On random graphs i. *Publicationes Mathematicae-Debrecen*, 6:290–297, 1959.

[19] J. Fan and R. L. Variable selection via nonconcave penalized likelihood and its oracle properties. *Journal of American Statistical Association*, pages 1348–1360, 2001.

[20] J. Fan and R. Li. Variable selection via nonconcave penalized likelihood and its oracle properties. *Journal of American Statistical Association*, pages 1348–1360, 2001.

[21] R. Fattal, D. Lischinski, and M. Werman. Gradient domain high dynamic range compression. *ACM Transactions on Graphics*, 21(3):249–256, 2002.

[22] R. T. Frankot, R. Chellappa, and S. Member. A method for enforcing integrability in shape from shading algorithms. *IEEE Transactions on Pattern Analysis and Machine Intelligence*, 10:439–451, 1988.

[23] I. Gannaz. Robust estimation and wavelet thresholding in partial linear models. *Statistics and Computing*, 17:293–310, 2007. arXiv:math/0612066v1.

[24] Y. Grandvalet, C. Ambroise, and J. Chiquet. Sparsity by worst-case quadratic penalties. 2012. arXiv:1210.2077.

[25] D. Harville. The use of linear model methodology to rate high school or college football teams. *Journal of American Statistical Association*, 72:278–289, 1977.

[26] B. K. P. Horn and M. J. Brooks. *Shape from Shading*. MIT Press, 1989.

[27] P. J. Huber. Robust regression: Asymptotics, conjectures and monte carlo. *The Annals of Statistics*, 1(5):799–821, 1973.

[28] P. J. Huber. *Robust Statistics*. New York: Wiley, 1981.

[29] X. Jiang, L.-H. Lim, Y. Yao, and Y. Ye. Statistical ranking and combinatorial Hodge theory. *Mathematical Programming*, 2010.

[30] M. Kahle. Topology of random clique complexes. *Discrete Mathematics*, 309:1658–1671, 2009.

[31] M. Kahle. Sharp vanishing thresholds for cohomology of random flag complexes. *Annals of Mathematics*, 2014. preprint, arXiv:1207.0149.

[32] J. Kleinberg. Authoritative sources in a hyperlinked environment. *Journal of the ACM*, 46(5):604–632, 1999.

[33] W. Ma, J. M. Morel, S. Osher, and A. Chien. An L_1-based variational model for retinex theory and its application to medical images. In *IEEE Conference on Computer Vision and Pattern Recognition*, pages 153–160, 2011.

[34] S. Negahban, S. Oh, and D. Shah. Iterative ranking from pair-wise comparisons. In *In Advances in Neural Information Processing Systems*, pages 2483–2491, 2012.

[35] G. Noether. Remarks about a paired comparison model. *Psychometrika*, 25:357–367, 1960.

[36] S. Osher, F. Ruan, J. Xiong, Y. Yao, and W. Yin. Noisy sparsity recovery via differential equations. *preprint*, 2014.

[37] B. Osting, J. Darbon, and S. Osher. Statistical ranking using the l_1-norm on graphs. *AIMS Journal on Inverse Problems and Imaging*, 7(3):907–926, 2013.

[38] D. Parikh and K. Grauman. Relative attributes. In *IEEE International Conference on Computer Vision*, pages 503–510, 2011.

[39] M. Penrose. *Random Geometric Graphs (Oxford Studies in Probability)*. Oxford University Press, 2003.

[40] P. E. H. R. O. Duda and D. G. Stork. *Pattern Classification*. John Wiley and Sons, 2001.

[41] A. Rajkumar and S. Agarwal. A statistical convergence perspective of algorithms for rank aggregation from pairwise data. In *International Conference on Machine Learning*, page preprint, 2014.

[42] H. Robbins and S. Monro. A stochastic approximation method. *The Annals of Mathematical Statistics*, 22(3):400–407, 1951.

[43] D. G. Saari. *Basic geometry of voting*. Springer, 1995.

[44] T. L. Saaty. A scaling method for priorities in hierarchical structures. *Journal of Mathematical Psychology*, 15(3):234–281, 1977.

[45] Y. She and A. B. Owen. Outlier detection using nonconvex penalized regression. *Journal of the American Statistical Association*, 106(494):626–639, 2011.

[46] A. Singer. Angular synchronization by eigenvectors and semidefinite programming. *Applied and Computational Harmonic Analysis*, 30(1):20–36, 2011.

[47] Y. Sismanis. How i won the "chess ratings – elo vs. the rest of the world" competition. *http://arxiv.org/abs/1012.4571v1*, 2010.

[48] D. Spielman and S.-H. Teng. Nearly-linear time algorithms for graph partitioning, graph sparsification, and solving linear systems. Proceedings of the thirty-sixth annual ACM symposium on Theory of computing, 2004.

[49] D. G. J. X. Stanley Osher, Martin Burger and W. Yin. An iterative regularization method for total variation-based image restoration. *SIAM Journal on Multiscale Modeling and Simulation*, 4(2):460–489, 2005.

[50] R. T. Stefani. Football and basketball predictions using least squares. *IEEE Transactions on Systems, Man, and Cybernetics*, 7:117–121, 1977.

[51] T. Sun and C. Zhang. Scaled sparse linear regression. *Biometrika*, 99(4):879–898, 2012.

[52] L. Thurstone. A law of comparative judgement. *Psychological Review*, 34:278–286, 1927.

[53] R. Tibshirani. Regression shrinkage and selection via the lasso. *Journal of the Royal Statistical Society, Series B*, 58(1):267–288, 1996.

[54] M. J. Wainwright. Sharp thresholds for high-dimensional and noisy sparsity recovery using l_1-constrained quadratic programming (lasso). *IEEE Transactions on Information Theory*, 55(5):2183–2202, 2009.

[55] D. Watts and S. Strogatz. Collective dynamics of 'small-world' networks. *Nature*, (393):440–442, 1998.

[56] N. Wormald. Models of random regular graphs. pages 239–298. In Surveys in Combinatorics, 1999.

[57] C.-C. Wu, K.-T. Chen, Y.-C. Chang, and C.-L. Lei. Crowdsourcing multimedia QoE evaluation: A trusted framework. *IEEE Transactions on Multimedia*, 15(5):1121–1137, 2013.

[58] J. Xiong, X. Cheng, and Y. Yao. Robust ranking on graphs. *Journal of Machine Learning Research, submitted*, 2013.

[59] Q. Xu, Q. Huang, T. Jiang, B. Yan, W. Lin, and Y. Yao. HodgeRank on random graphs for subjective video quality assessment. *IEEE Transactions on Multimedia*, 14(3):844–857, 2012.

[60] Q. Xu, Q. Huang, and Y. Yao. Online crowdsourcing subjective image quality assessment. pages 359–368. ACM Multimedia, 2012.

[61] Q. Xu, T. Jiang, Y. Yao, Q. Huang, B. Yan, and W. Lin. Random partial paired comparison for subjective video quality assessment via HodgeRank. pages 393–402. ACM Multimedia, 2011.

[62] Q. Xu, J. Xiong, Q. Huang, and Y. Yao. Robust evaluation for quality of experience in crowdsourcing. pages 43–52. ACM Multimedia, 2013.

[63] Q. Xu, J. Xiong, Q. Huang, and Y. Yao. Online hodgerank on random graphs for crowdsourceable QoE evaluation. *IEEE Transactions on Multimedia*, 16(2):373–386, 2014.

[64] W. Yin, S. Osher, J. Darbon, and D. Goldfarb. Bregman iterative algorithms for compressed sensing and related problems. *SIAM Journal on Imaging Sciences*, 1(1):143–168, 2008.

[65] S. X. Yu. Angular embedding: from jarring intensity differences to perceived luminance. In *IEEE Conference on Computer Vision and Pattern Recognition*, pages 2302–2309, 2009.

[66] S. X. Yu. Angular embedding: A robust quadratic criterion. *IEEE Transactions on Pattern Analysis and Machine Intelligence*, 34(1):158–173, 2012.

[67] K. Yuan, Q. Ling, W. Yin, and A. Ribeiro. A Linearized Bregman Algorithm for Decentralized Basis Pursuit. *EUSIPCO*, 2013.

SUPPLEMENTARY MATERIAL: PROOFS OF THEOREMS

Proof of Theorem 1: The theorem mainly follows the Theorem 1 in [54] by changing the notation from $X, \beta, n, p, \gamma, \lambda_n$ to $\Psi, \gamma, l, m, \eta, \lambda/l$. Note that in [54], column normalization $\mu_\Psi = 1$ is assumed, while in this paper we keep this parameter $\mu_\Psi \leq 1$. Our results here assume Gaussian noise, which can be extended to sub-Gaussian noise in [54] resulting to a slight different λ up to a constant $\sqrt{2}$ as well as a different constant in l_∞ bound. □

Proof of Theorem 2: Here we present a self-contained sketchy proof, leaving the readers to [36] for a full development of the related theory.

(No-false-positive) First consider the LBI restricted on S

$$(p_S^{k+1} + \gamma_S^{k+1}/\kappa) - (p_S^k + \gamma_S^k/\kappa) = \Psi_S^T \Psi_S (\tilde{\gamma}_S - \gamma_S^k) \triangle t \tag{15}$$

where $\tilde{\gamma}_S = \gamma_S^* + (\Psi_S^T \Psi_S)^{-1} \Psi_S^T \Psi \epsilon$.

Note that $\|\Psi_S(\tilde{\gamma}_S - \gamma^k)\|$ is monotonically decreasing under the condition $h\|\Psi_S^T \Psi_S\| < 2$. In fact,

$$\begin{aligned}
& \|\Psi_S(\tilde{\gamma}_S - \gamma^{k+1})\|^2 - \|\Psi_S(\tilde{\gamma}_S - \gamma^k)\|^2 \\
= \; & \|\Psi_S(\gamma^{k+1} - \gamma^k)\|^2 + 2(\gamma^{k+1} - \gamma^k)^T \Psi_S^T \Psi_S (\gamma^k - \tilde{\gamma}_S) \\
= \; & \|\Psi_S(\gamma^{k+1} - \gamma^k)\|^2 - 2/\triangle t (\gamma^{k+1} - \gamma^k)^T \dots \\
& \cdot [(p_S^{k+1} - p_S^k) + (\gamma_S^{k+1}/\kappa - \gamma_S^k/\kappa)] \\
\leq \; & \|\Psi_S(\gamma^{k+1} - \gamma^k)\|^2 \dots \\
& -2/\triangle t (\gamma^{k+1} - \gamma^k)^T (\gamma_S^{k+1}/\kappa - \gamma_S^k/\kappa) \\
= \; & (\gamma^{k+1} - \gamma^k)^T (\Psi_S^T \Psi_S - 2/h)(\gamma^{k+1} - \gamma^k) \\
\leq \; & 0,
\end{aligned}$$

where we have used $(\gamma^{k+1} - \gamma^k)^T ((p_S^{k+1} - p_S^k) \geq 0$ since $\gamma_i(p_i - p_i') = |\gamma_i| - \gamma_i p_i' \geq 0$. Using this fact, we can roughly see γ_S^k is bounded. Actually,

$$\begin{aligned}
\|\gamma_S^k\|_\infty &\leq \|\tilde{\gamma}_S\|_\infty + \|\tilde{\gamma}_S - \gamma_S^k\|_2 \\
&\leq \|\tilde{\gamma}_S\|_\infty + \frac{\|\Psi_S(\tilde{\gamma}_S - \gamma_S^k)\|_2}{\sqrt{l C_{min}}} \\
&\leq \|\tilde{\gamma}_S\|_\infty + \frac{\|\Psi_S(\tilde{\gamma}_S - \gamma_S^0)\|_2}{\sqrt{l C_{min}}}.
\end{aligned}$$

Using concentration inequality, we can bound the last term by B with high probability (at least $1 - 1/(m\sqrt{\log m}) - 1/(n\sqrt{\log n})$ via a Gaussian tail bound).

Now we turn to the LBI restricted on $T = S^c$ with γ_S^k above.

$$\begin{aligned}
& (p_T^{k+1} + \gamma_T^{k+1}/\kappa) - (p_T^k + \gamma_T^k/\kappa) \\
= \; & \Psi_T^T \Psi_S (\gamma_S^* - \gamma_S^k) \triangle t + \Psi_T^T \Psi \epsilon \\
= \; & \Psi_T^T \Psi_S^\dagger [(p_S^{k+1} - p_S^k) + (\gamma_S^{k+1}/\kappa - \gamma_S^k/\kappa)] + \Psi_T^T P_T \Psi \epsilon
\end{aligned}$$

where $P_T = I - P_S = I - \Psi_S^\dagger \Psi_S^T$ is the projection matrix onto $\mathrm{im}(\Psi_T)$.

A telescope sum on both sides with $p^0 = \gamma^0 = 0$,

$$p_T^k + \gamma_T^k/\kappa = \Psi_T^* \Psi_S^\dagger (p_S^k + \gamma_S^k/\kappa) + t_k \Psi_T^* P_T \Psi \epsilon.$$

Now consider the l_∞-norm of the right side. If it is smaller than 1, then $\gamma_T^k = 0$ which implies no-false-positive. Note that the first part

$$\begin{aligned}
\|\Psi_T^* \Psi_S^\dagger (p_S^k + \gamma_S^k/\kappa)\|_\infty &\leq (1-\eta)(1 + \|\gamma_S^k\|_\infty/\kappa) \\
&\leq 1 - (1 - B/\kappa\eta)\eta
\end{aligned}$$

Also we have $\|\Psi_T^T P_T \Psi \epsilon\| \leq 2\sigma\mu_\Psi \sqrt{\log m/l}$ with high probability (at least $1 - 1/(m\sqrt{\log m})$ via a Gaussian tail bound), so when $t^k \leq \bar{\tau}$, the second term is smaller than $(1 - B/\kappa\eta)\eta$. Hence the whole term is less than 1, as desired.

(Sign-consistency) Given no-false-positive before $\bar{\tau}$, to achieve sign consistency, we only need to show (15) can achieve no-false-negtive before $\bar{\tau}$.

Denote $\Phi_k = |\tilde{\gamma}_S| - |\gamma_S^k| - < p_S^k, \tilde{\gamma}_S - \gamma_S^k > + \frac{||\tilde{\gamma}_S - \gamma_S^k||^2}{2\kappa}$ and

$$F(x) = \frac{x}{2\kappa} + \begin{cases} 0 & 0 \leq x < \tilde{\gamma}_{min}^2 \\ 2x/\tilde{\gamma}_{min} & \tilde{\gamma}_{min}^2 \leq x \leq s\tilde{\gamma}_{min}^2 \\ 2\sqrt{xs} & x \geq s\tilde{\gamma}_{min}^2 \end{cases} \tag{16}$$

which is monotonically nondecreasing and right continuous. Then $F(||\tilde{\gamma}_S - \gamma_S^k||^2) \geq \Phi_k$, or equivalently $||\tilde{\gamma}_S - \gamma_S^k||^2 \geq F^{-1}(\Phi_k)$, where F^{-1} is the right-continuous inverse of F.

Next we are going to show Φ_k is decreasing at least

$$\Phi_{k+1} - \Phi_k \leq -\triangle t \tilde{C}_{min} F^{-1}(\Psi_k). \tag{17}$$

where $\tilde{C}_{min} = C_{min} l(1 - h\|\Psi_S \Psi_S^T\|/2)$. With a sufficient fast drop of Φ_k, we just need to show $\Phi_k \leq \tilde{\gamma}_{min}^2/(2\kappa)$, which is sufficient for no-false-negative, i.e., every outlier in S has been found by γ_k.

Multiplying $\tilde{\gamma}_S - \gamma_S^k$ on the both sides of (15), gives

$$\begin{aligned}
& \Phi_{k+1} - \Phi_k + (p_S^{k+1} - p_S^k)\gamma_S^k - \|\gamma_S^{k+1} - \gamma_S^k\|^2/2\kappa \\
= \; & -\triangle t \left\langle \tilde{\gamma}_S - \gamma_S^k, \Psi_S^T \Psi_S (\tilde{\gamma}_S - \gamma_S^k) \right\rangle
\end{aligned}$$

Since for $i \in S$, $(p_i^{k+1} - p_i^k)\gamma_i^{k+1} = |\gamma_i^{k+1}| - p_i^k \gamma_i^{k+1} \geq 0$,

$$\begin{aligned}
& \|\gamma_S^{k+1} - \gamma_S^k\|^2/\kappa - 2(p_S^{k+1} - p_S^k)\gamma_S^k \\
\leq \; & \|\gamma_S^{k+1} - \gamma_S^k\|^2/\kappa + 2(p_S^{k+1} - p_S^k)(\gamma_S^{k+1} - \gamma_S^k) \\
\leq \; & \|\gamma_S^{k+1} - \gamma_S^k\|^2/\kappa + 2(p_S^{k+1} - p_S^k)(\gamma_S^{k+1} - \gamma_S^k) \\
& + \kappa \|p_S^{k+1} - p_S^k\|^2 \\
\leq \; & \kappa \|p_S^{k+1} - p_S^k + (\gamma_S^{k+1} - \gamma_S^k)/\kappa\|^2 \\
= \; & \kappa \triangle t^2 \|\Psi_S^T \Psi_S (\tilde{\gamma}_S - \gamma_S^k)\|^2
\end{aligned}$$

So for $h = \kappa \triangle t$,

$$\begin{aligned}
& \Phi_{k+1} - \Phi_k \\
\leq \; & -\triangle t \left\langle \Psi_S(\tilde{\gamma}_S - \gamma_S^k), \Psi_S(\tilde{\gamma}_S - \gamma_S^k) \right\rangle \\
& + \frac{\kappa \triangle t^2}{2} \left\langle \Psi_S^T \Psi_S (\tilde{\gamma}_S - \gamma_S^k), \Psi_S^T \Psi_S (\tilde{\gamma}_S - \gamma_S^k) \right\rangle \\
= \; & -\triangle t \left\langle \Psi_S(\tilde{\gamma}_S - \gamma_S^k), (I - h\Psi_S^T \Psi_S/2) \Psi_S (\tilde{\gamma}_S - \gamma_S^k) \right\rangle \\
\leq \; & -\triangle t (1 - h\|\Psi_S^T \Psi_S\|/2) \|\Psi_S(\tilde{\gamma}_S - \gamma_S^k)\|^2 \\
\leq \; & -\triangle t C_{min} l (1 - h\|\Psi_S^T \Psi_S\|/2) \|\tilde{\gamma}_S - \gamma_S^k\|^2 \\
\leq \; & -\triangle t C_{min} l (1 - h\|\Psi_S^T \Psi_S\|/2) F^{-1}(\Psi_k)
\end{aligned}$$

which gives (17).

Now (17) means $\triangle t \leq \tilde{C}_{min}(\Phi_k - \Phi_{k+1})/F^{-1}(\Phi_k)$. Let $L_k = F^{-1}(\Phi_k)$. The following gives a piecewise bound

$$\frac{\Phi_k - \Phi_{k+1}}{F^{-1}(\Phi_k)} \leq \begin{cases} (\frac{\log L_k}{2\kappa} - 2\sqrt{\frac{s}{L_k}}) - (\frac{\log L_{k+1}}{2\kappa} - 2\sqrt{\frac{s}{L_{k+1}}}), \\ \quad \text{if } L_k > s\tilde{\gamma}_{min}^2 \\ (\frac{1}{2\kappa} + \frac{2}{\tilde{\gamma}_{min}})(\log L_k - \log L_{k+1}), \\ \quad \text{if } s\tilde{\gamma}_{min}^2 \geq L_k > \tilde{\gamma}_{min}^2 \\ \frac{\Phi_k - \Phi_{k+1}}{\tilde{\gamma}_{min}^2}, \text{if } L_k = \tilde{\gamma}_{min}^2, \Phi_k > \tilde{\gamma}_{min}^2/(2\kappa) \end{cases} \tag{18}$$

Now a telescope sum of the right hand gives an upper bound

$$\begin{aligned} \tau_1 &:= \inf\{t^k > 0 : \Phi_k \leq \tilde{\gamma}_{min}^2/(2\kappa)\} \\ &\leq \frac{4 + 2\log s}{\tilde{C}_{min}\tilde{\gamma}_{min}} + \frac{1}{\kappa\tilde{C}_{min}} \log(\frac{\|\tilde{\gamma}\|_2}{\tilde{\gamma}_{\min}}) + 3\triangle t. \end{aligned}$$

The condition $\gamma_{\min} \geq \frac{4\sigma}{C_{min}^{1/2}}\sqrt{\frac{\log m}{l}}$ and concentration of gaussian noise guarantee $|\tilde{\gamma}_i - \gamma_i| < \gamma_{min}/2 \leq |\gamma_i|/2, \ \forall i$. Using this equation to replace $\tilde{\gamma}$ with γ and setting $\tau_1 \leq \bar{\tau}$, we could obtain the sign-consistency condition.

(l_2-bound) The proof is similar to that of sign-consistency. Using the inequality

$$\Phi_{k+1} - \Phi_k \leq -\tilde{C}_{min}\triangle t \max(\tilde{F}^{-1}(\Phi_k), \|\tilde{\gamma}_S - \gamma_S^k\|^2)$$

where $\tilde{F}(x) = \frac{x}{2\kappa} + 2\sqrt{xs} \geq F(x)$, so $\tilde{F}^{-1}(x) \leq F^{-1}(x)$. Let $\tilde{L}_k = \tilde{F}^{-1}(\Phi_k)$. We get the following bound

$$\tilde{C}_{min}\triangle t \leq \begin{cases} \frac{\log \tilde{L}_k - \log \tilde{L}_{k+1}}{2\kappa} - 2\sqrt{s}(\frac{1}{\sqrt{\tilde{L}_k}} - \frac{1}{\sqrt{\tilde{L}_{k+1}}}) \\ \quad \text{if } \Phi_k \geq \tilde{F}(C^2 s\log m/l) \\ \frac{\Phi_k - \Phi_{k+1}}{C^2 s\log m/l}, \text{if } \Phi_k < \tilde{F}(C^2 s\log m/l) \end{cases} \tag{19}$$

A telescope sum of the right hand gives an upper bound

$$\begin{aligned} \tau_2(C) &:= \inf\{t^k > 0 : ||\gamma_k - \tilde{\gamma}||_2 \leq C\sqrt{\frac{s\log m}{l}}\} \\ &\leq \frac{1}{2\kappa\tilde{C}_{min}}(1 + \log\frac{l|\tilde{\gamma}|_2^2}{C^2 s\log m}) \\ &\quad + \frac{4}{C\tilde{C}_{min}}\sqrt{\frac{l}{\log m}} + 2\triangle t. \end{aligned}$$

The result follows from setting $\tau_2(C) \leq \bar{\tau}$. □